Available online at www.sciencedirect.com
SCIENCE DIRECT®
ELSEVIER
Earth and Planetary Science Letters 216 (2003) 259–269
EPSL
www.elsevier.com/locate/epsl

Seismic scattering at the top of the mantle Transition Zone

H. Thybo [a,*], L. Nielsen [a], E. Perchuc [b]

[a] Geological Institute, University of Copenhagen, Øster Voldgade 10, 1350 Copenhagen K, Denmark
[b] Institute of Geophysics, Polish Academy of Sciences, ul. Księcia Janusza 64, PL-01452 Warsaw, Poland

Received 21 March 2003; received in revised form 28 July 2003; accepted 15 August 2003

Abstract

We document strong seismic scattering from around the top of the mantle Transition Zone in all available high resolution explosion seismic profiles from Siberia and North America. This seismic reflectivity from around the 410 km discontinuity indicates the presence of pronounced heterogeneity in the depth interval between 320 and 450 km in the Earth's mantle. We model the seismic observations by heterogeneity in the form of random seismic scatterers with typical scale lengths of kilometre size (10–40 km by 2–10 km) in a 100–140 km thick depth interval. The observed heterogeneity may be explained by changes in the depths to the α–β–γ spinel transformations caused by an unexpectedly high iron content at the top of the mantle Transition Zone. The phase transformation of pyroxenes into the garnet mineral majorite probably also contributes to the reflectivity, mainly below a depth of 400 km, whereas we find it unlikely that the presence of water or partial melt is the main cause of the observed strong seismic reflectivity. Subducted oceanic slabs that equilibrated at the top of the Transition Zone may also contribute to the observed reflectivity. If this is the main cause of the reflectivity, a substantial amount of young oceanic lithosphere has been subducted under Siberia and North America during their geologic evolution. Subducted slabs may have initiated metamorphic reactions in the original mantle rocks.

Keywords: mantle; transition zone; 410 km discontinuity; seismic reflectivity; heterogeneity

1. Introduction

The 410 km discontinuity ('410') is one of the major boundaries in the Earth's interior, marking the top of the mantle Transition Zone, which is bounded by strong vertical changes in seismic velocity and characterised by a high vertical velocity gradient. It is heavily debated whether the mantle Transition Zone between the 410 km and 660 km discontinuities forms an impenetrable boundary to subducting lithospheric slabs from the surface of the Earth and to rising thermal plumes from the deep mantle [1–3]. The current understanding of the Transition Zone is primarily in terms of metamorphic phase transitions in an isochemical mantle dominated by olivine [4,5], although chemical changes cannot be ruled out [6,7]. The '410' has been interpreted seismically as a sharp interface at slightly variable depths between 390 and 430 km, inversely related to temperature. This

* Corresponding author. Tel.: +45-3532-2452; Fax: +45-3314-8322.
E-mail addresses: thybo@geol.ku.dk (H. Thybo), ln@geo.geol.ku.dk (L. Nielsen), per@igf.edu.pl (E. Perchuc).

0012-821X/03/$ – see front matter
doi:10.1016/S0012-821X(03)00485-0

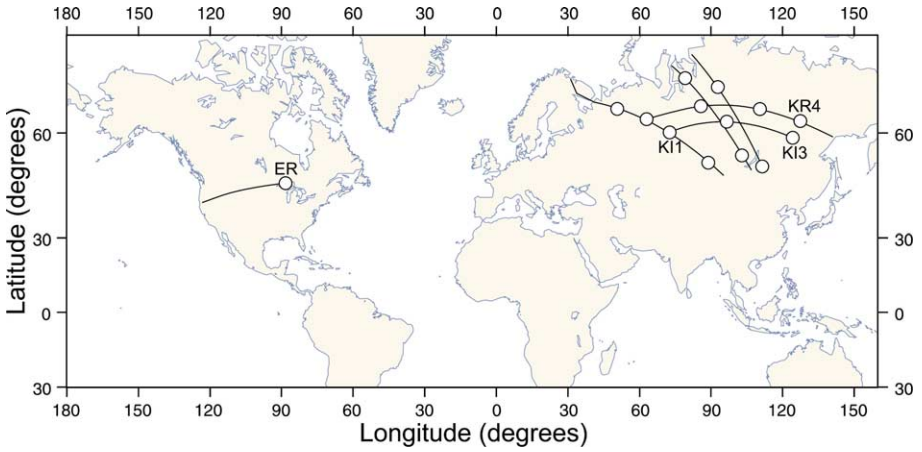

Fig. 1. Map showing the seismic profiles for which the observed seismic record sections show the scattered waves from the top of the mantle Transition Zone. The full lines indicate the seismic lines and the circles show the locations of the shot points. The seismic sections illustrated in Figs. 2 and 3 are for the labelled shot points; for Peaceful Nuclear Explosion (PNE) sections: KR4 = KRATON shot point 4, KI1 and KI3 = KIMBERLITE shot points 1 and 3, as well as for ER = The Early Rise shot point.

roughly coincides with the depth at which the transformation of olivine (α) to β spinel occurs [8,9].

Petrologic models of the phase transformation indicate that the '410' should be a transitional interval, which is at least 10–20 km thick [10,11], whereas interpretations of earthquake seismological data usually indicate a narrow zone which may be less than 6 km thick [12,13]. Thermodynamic calculations show that the olivine to β spinel transformation may take place over a less than 10 km thick interval [14,15], although other constituents of the mantle rocks will tend to make the transition less distinct. Most seismological interpretations of the fine structure of the '410' are based on underside reflections and P to S conversions of teleseismic waves from distant earthquakes [12,13,16,17], but reflections have also been identified from above the '410' [18–20]. We present long-range seismic sections from near-surface explosion sources that show clear seismic phases from the depth interval around the '410' at offsets of 1500–2500 km from the seismic sources. The recordings are sampled at high density (10–20 km spacing between seismometers) along profiles on the Earth's surface, and the high frequency content (centre frequency of 2–4 Hz) is higher than in most other available seismological data that sample the mantle at similar depths.

2. Seismic observations

We find that all the available controlled-source, long-range seismic sections from Siberia and North America show pronounced seismic reflectivity from around the '410' (Fig. 1). This indicates the presence of a heterogeneous interval of 100–140 km thickness around the top of the Transition Zone, as well as variation in depth to the '410' reflector. In most seismic sections, the P_{410} reflection from the '410' is the strongest seismic phase in the offset interval of ~1600 km to ~2000 km, but there is an earlier seismic phase, P_{320}, which is reflected from around 310–350 km depth. This phase is clearly identifiable in all available high density record sections at ~1800 km to ~2400 km offset and marks the onset of the strong reflectivity (Figs. 2 and 3). The relation between the P_{410} and the P_{320} in the long-range seismic sections is qualitatively similar to the relation between the reflections from the Moho and the top of the reflective lower crust in crustal, wide-angle seismic sections [21], except for the obvious huge differences in offset and travel

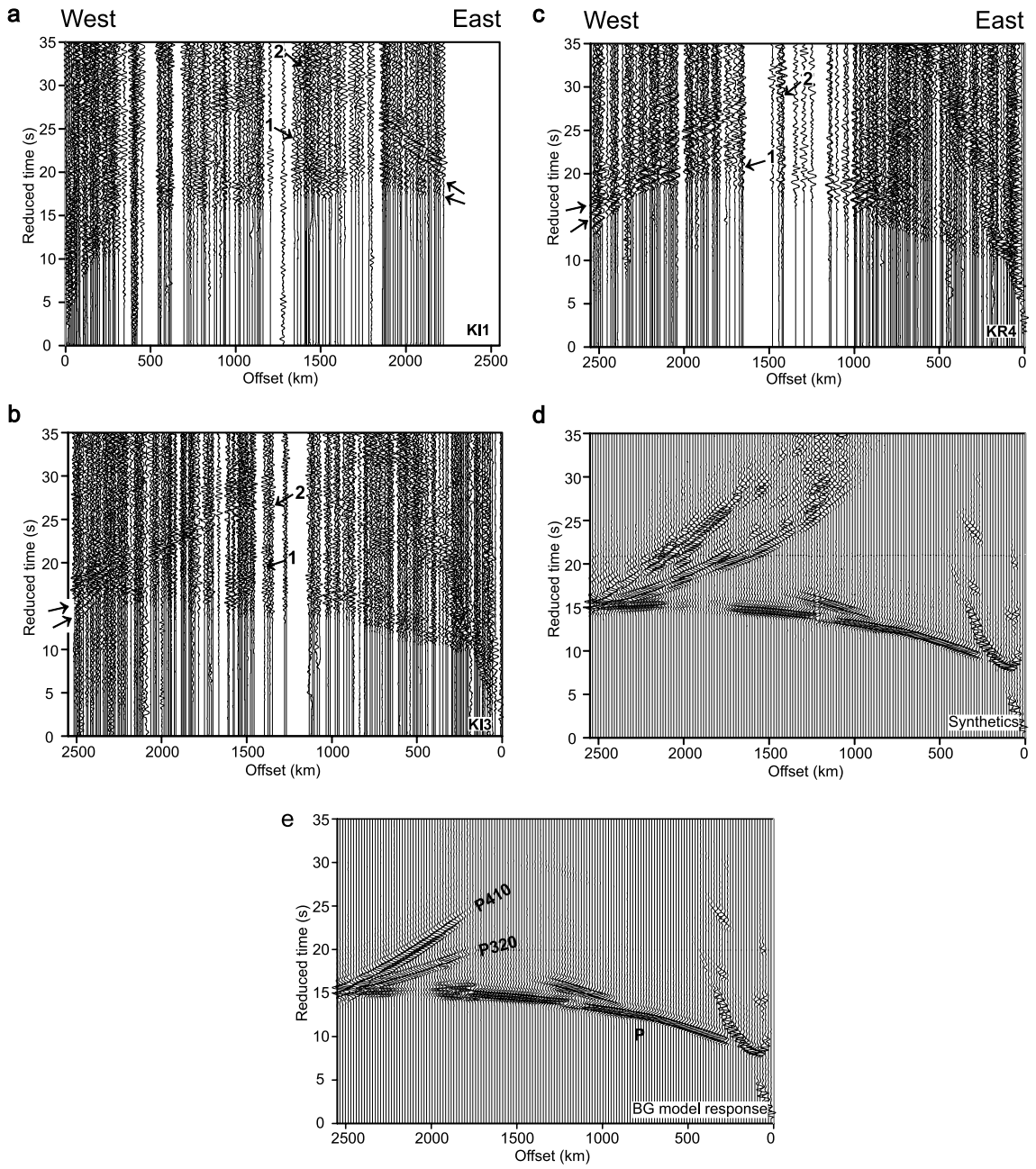

Fig. 2. Trace-normalised seismic sections plotted in reduced travel time versus offset from the seismic source with a reduction velocity of 8.7 km/s. (a–c) KI1, KI3, and KR4 refer to PNE sections KIMBERLITE 1, 2 and KRATON 4. The onset of the seismic reflectivity from around the top of the Transition Zone (P_{320}) is marked by the No. 1 arrows, and the P_{410} reflection from the '410' is marked by the No. 2 arrows. (d,e) The calculated 2D visco-elastic finite-difference waveform responses of the models (shown in Fig. 4). The source used for the synthetic sections is a Ricker wavelet with a central frequency of 2 Hz. The calculated seismograms have been convolved with the instrument response of the seismometers. (d) 'Synthetics' is for the preferred model in Fig. 4c. (e) 'BG model response' is for the background velocity model in Fig. 4a. The synthetic seismograms are similar for all shallow events, whereas they are different for the far offset, late arrivals from the top of the Transition Zone.

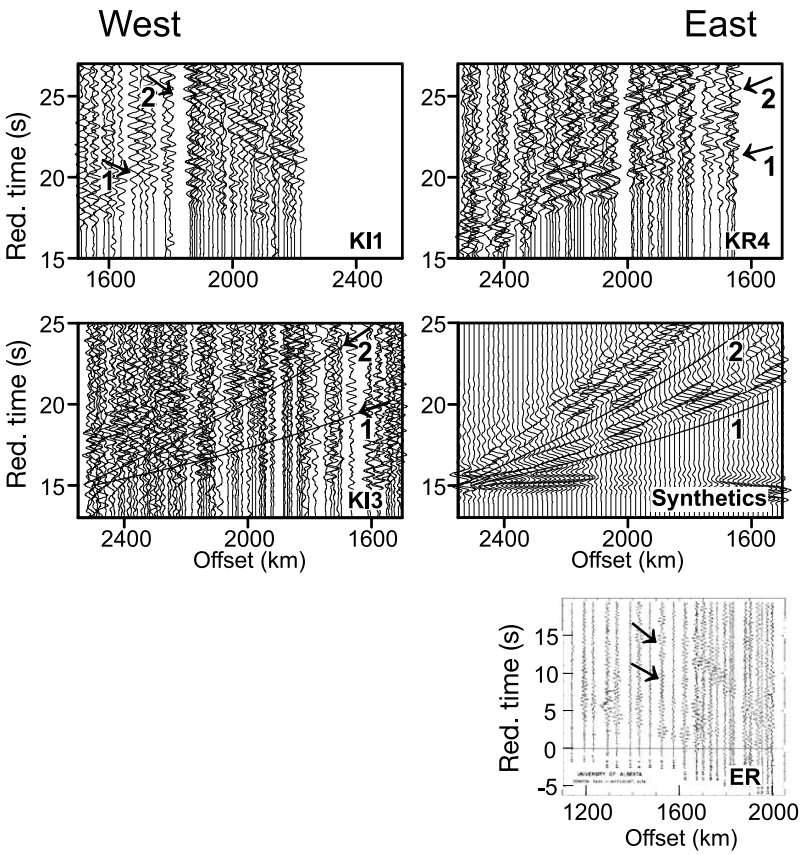

Fig. 3. Close-ups of the sections illustrated in Fig. 2 together with a close-up of a record section from the Early Rise experiment in North America (ER). The reduction velocities are 8.7 km/s for the PNE sections and 8.0 km/s for ER profile 6. Travel time curves are calculated for reflections from gradient zones at depths of 310–330 km (P_{320}) and 400–430 km (P_{410}) (cf. Fig. 4). Tilted arrows show the interpreted onset of the P_{320} (1) and P_{410} (2) reflections.

time. The best available examples of the seismic reflectivity at the top of the Transition Zone are in data from the Soviet 'Peaceful Nuclear Explosions' (PNE) seismic sections, which were recorded during the period of 1965–1988 to investigate primarily the upper mantle structure [22].

We have identified the same type of reverberative reflectivity from around the top of the Transition Zone in all eight PNE seismic sections with the necessary offset of more than 2000 km, which are available to us. Reversed sections show similar features, but with small differences in amplitude characteristics in the two directions. Kinematic modelling of the observed travel times from Siberia shows that the two main phases define a zone of ~100 km thickness at a depth of around 400 km. The upper interface, modelled as a 20 km thick velocity change around a depth of 320 km, corresponds to the onset of the strong seismic reflectivity (P_{320}). The '410' reflector is a ~30 km thick gradient zone at a depth of 400–430 km, which is very deep for an area with low heat flow. The ~30 km thick transition is required instead of an abrupt interface in order to explain the absence of a '410' reflection at offsets less than 1500 km. The preferred synthetic seismic section (Figs. 2d and 3) resembles the observations qualitatively. Comparison to the synthetic section (Fig. 2e), calculated for the background model (without heterogeneity, Fig. 4a), clearly

demonstrates the need for the pronounced heterogeneity around the top of the Transition Zone in order to explain the seismic observations.

Chemical explosions can also generate sufficiently strong seismic energy to reveal this reflectivity above the ambient noise. Data from the Early Rise seismic experiment in North America, resulting from detonation of charges consisting of 30 tonnes of explosives in Lake Superior, indicates the presence of two reflectors at depths of ~350 km and ~450 km along the west-striking profile 6 [23]. The analysis by Lewis and Meyer of the primary amplitudes of the P_{320} phase suggests that the upper reflector is a ~20 km thick zone with a change in velocity of 0.25 km/s, and that the deeper reflection (P_{410}) is from a first order discontinuity with a jump in velocity of 0.6 km/s [23]. It is remarkable that this interpretation shows a very deep '410' reflector at c. 450 km depth. Our analysis of other seismic sections from the same experiment has identified similar features and depths. Kinematic interpretation of observations on the permanent seismological network in North America of the 1997 earthquake at El Paso, Texas [24], indicates that the '410' is deep in eastern North America and shallower in western North America which is contrary to the depth that would be expected from the low heat flow [25]. Hence, there is a risk that the P_{320} reflection may be interpreted as the P_{410} reflection, which may lead to serious misinterpretation of the depth to the top of the mantle Transition Zone.

The amplitude variation with offset shows abrupt increases for both the P_{320} and the P_{410} reflections at ~1800 and ~1600 km, respectively. We ascribe this amplitude increase to critically reflected waves, suggestive of positive velocity contrasts at both boundaries. However, analysis of multiply reflected ScS phases from the Earth's core has previously identified an interface at c. 330 km in eastern Siberia with a negative reflection coefficient, indicative of a velocity reversal [26]. The frequency content of the PNE data (up to 6 Hz) is about one order of magnitude higher than for the global earthquake observations used for the ScS analysis. Hence the PNE data show the fine-scale reflectivity at short wavelength, which may identify the top of the reflective zone as a positive velocity contrast. The ScS analysis primarily shows the long wavelength characteristics of the reflecting depth interval, which could correspond to a negative velocity contrast.

3. Seismic modelling

We explain the seismic reflectivity from around the top of the Transition Zone as reflections from small-scale heterogeneity in the 320–450 km depth range. We have calculated full waveform synthetic seismograms for one-dimensional, spherical models of the Earth and for two-dimensional viscoelastic finite-difference models in order to simulate the effects of wave propagation in heterogeneous media [27]. We estimate the effects of the velocity (and density) variations on the seismic data by the method described by Nielsen et al. [28]. Random fluctuations described by their distribution function, standard deviation and spatial correlation lengths were superimposed on a background velocity structure, which was constrained by kinematic modelling of the observed travel times [20,29]. The background velocities are larger than in the global models of upper mantle velocity (e.g. the IASPEI model [30]) as expected for the cold Siberian craton. Synthetic seismograms for one-dimensional models, with typical layer thicknesses on the order of 10 km both above and below the '410', adequately describe the general characteristics of the reflectivity, except that strong lateral correlation in the synthetic reflections, induced by the modelling algorithm, is inconsistent with the observations. We investigated many models by 1D modelling. They all indicate that the gradient zone around 410 km depth is smoother than the surrounding intervals. We therefore have chosen to keep a smooth, c. 30 km thick, gradient zone at the 410 km discontinuity in the investigated 2D models, even though this feature is not well resolved by the data.

The synthetic seismic section (Fig. 2e) for the background model (Fig. 4a) shows the main phases that were used for the modelling: the direct P, and the reflections (P_{320} and P_{410}) from the discontinuities or gradient zones at depths of 320 and 410 km. This section clearly shows that such

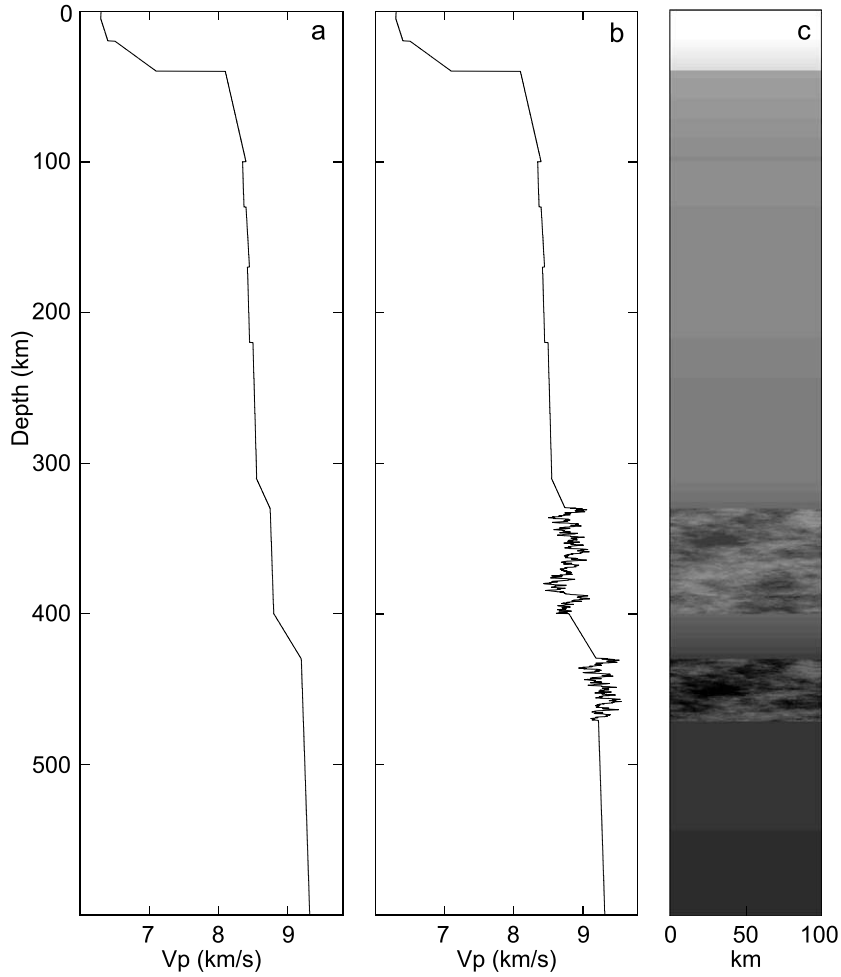

Fig. 4. (a) 1D background P-wave velocity model interpreted by kinematic modelling of travel times of the main seismic phases in the record sections. (b) 1D profile extracted from the 2D model in panel c. (c) Part (100 km horizontally) of the preferred 2D model, which explains the seismic scattering from the top of the mantle transition zone. The fluctuations above and below the '410' follow a von Karman distribution function with a Hurst number of 0.5 (exponential medium). The horizontal and vertical correlation lengths are 20 km and 5 km, respectively. The standard deviation of the fluctuations is 2% of the background velocity value. S-wave and density fluctuations are proportional to the P-wave fluctuations. The 2D model extends to 2500 km offset and 500 km depth. It is sampled at a grid spacing of 180 m (five grid points per minimum shear wavelength).

a simple model cannot explain the observed scattering in the seismic sections. Nevertheless, the main seismic reflections have the correct travel times, and the amplitude characteristics correspond to the amplitudes at the onset of the observed reflectivity.

The two-dimensional models of the heterogeneity are constructed assuming a von Karman distribution with a Hurst number of 0.5 for the seismic velocity fluctuations. Media described by a von Karman distribution function are relatively rough, because a broad range of wavenumbers contribute to the heterogeneity spectrum. Media described by a von Karman distribution function with a Hurst number of 0.5 are often referred to as exponential media. Such media show characteristics which are intermediate between smooth Gaussian media and fractal media. The Hurst number, which can take on a value between 0 and 1, controls the correlation decay. Small Hurst

numbers result in a more rapid decay than large Hurst numbers [31].

The synthetic seismograms are calculated by propagation of the wave field through a regular grid using a 2D visco-elastic, finite-difference algorithm [27]. The source is a Ricker wavelet with a centre frequency of 2 Hz. The grid spacing of 180 m ensures a minimum of five grid points per minimum shear wavelength in the 2500 km long and 500 km deep models. The 328 s long records are calculated in time steps of 6 ms in order to maintain stability of the finite-difference algorithm. Edge effects (i.e. reflections from the sides and the bottom of the model) are damped by a 30 km wide damping zone ($Q_p = Q_s = 2$), which is padded around the model grid. The upper boundary of the model is modelled as a free surface. Hence, about 50 million points are needed to define the grid, and the full wave field is propagated through the whole model in 55 000 time steps.

The synthetic seismic sections are similar to the observations (Figs. 2 and 3) for fluctuations (Fig. 4) with a standard deviation of $\sim$0.2 km/s and correlation lengths of 10–40 km (horizontally) and 2–10 km (vertically). The actual size of the scatterers is below the resolution limit of the seismic data and cannot be uniquely resolved. Models in which only the interval above the '410' contains scatterers reproduce the characteristic reflectivity in front of the P_{410} reflection but cannot explain the coda to the P_{410}, although multiply reflected waves generate weak signals after the '410' reflection. This shows that the upper part of the Transition Zone below the '410' is heterogeneous.

The seismic scattering around the '410' is only identifiable in high resolution seismic sections, which are recorded at high frequency and with dense spatial sampling. As a result of the short wavelengths, such data provide invaluable information about the fine structure of the deep part of the upper mantle around the top of the Transition Zone. Our velocity model is consistent with the results from global tomographic studies [1,32] and regional surface wave inversion and travel time tomography [29,33]. The seismic reflectivity from around the top of the Transition Zone may be explained by chemical changes, phase transformations, the presence of subducted oceanic slabs that equilibrated at this depth level, or, possibly, changes in fluid content, the presence of melts or other thermal effects.

4. Petrologic and tectonic implications

The presented seismic observations and results of our modelling indicate abrupt changes in the seismic velocity structure around the 410 km discontinuity. The seismic model includes a strong change in reflectivity, which indicates a pronounced change in composition, crystal orientation, or metamorphic state of the rocks. We find three plausible explanations for this feature.

(1) It is generally accepted that the '410' can be explained by the phase transformation of olivine (α) to β spinel in an isochemical mantle [4,8,9]. Measured and thermodynamically calculated pressure and temperature values for the transformation predict depths at around 410 km for an iron content of 10% (Fe# = 10, Fig. 5C). The Clapeyron slope is negative, such that the transformation is predicted to be shallower than 410 km at the low temperatures under Siberia and cratonic North America. The thickness of the transformation interval increases substantially with increasing iron content. For high Fe#, the full α–β–γ phase transition of spinel will take place in the reflective depth interval. The transformation is significant already from its onset (Fig. 5C). The maximum reported iron content is 12% in upper mantle xenoliths from depths shallower than 250 km. The few very deep xenoliths from around the Transition Zone indicate a highly varying iron content of 5–17.5%, depending on mineral type [34]. It is therefore possible that some of the mantle rocks below 250 km depth have a higher Fe content than in the shallow mantle. If these rocks contain 17% Fe, the multi-phase transformation (α–β–γ) will take place in the depth interval between 345 km at 1200°C and 483 km at 1600°C (calculated from values in [35]). The required temperatures are close to predicted geotherms for shield and platform areas. Hence, our seismic model is consistent with a high Fe# around the '410'. The observed heterogeneity will in this case

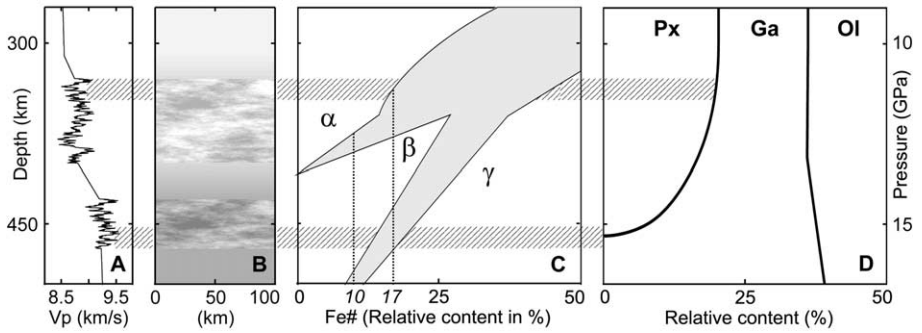

Fig. 5. Two metamorphic reactions in mantle rocks may cause the heterogeneity around the top of the mantle Transition Zone that may explain the observed seismic scattering. (A) Part of the vertical P-wave velocity profile extracted from the two-dimensional P-wave velocity model of which 100 km is shown in B. The velocity fluctuations are equivalent to the fluctuations shown in Fig. 4. Two types of metamorphic transformation may contribute to the seismic observations. (C) The α–β–γ spinel transformation of the olivine part of the mantle. Grey regions show transformation regions. The horizontal axis from 0 to 50% refers to the Fe# (the relative content of Fe compared to Mg). This model implies a variable iron content in the mantle; the diagram shows that the modelled depths are consistent with a Fe# of 17. (D) The transformation from pyroxene into the garnet phase majorite may also contribute to the observed reflectivity, in particular below the '410'. Heavy lines show the relative abundance of pyroxene (Px), garnet (Ga) and olivine (Ol) as a function of pressure (depth); note that the horizontal scale is for relative occurrences of 0 to 50%.

be explained by partial metamorphism of the olivine between the α, β and γ spinel phases. Further support for this model is found from the modelled, relatively deep increase in velocity, which takes place in the depth interval of 410 to 430 km, opposite to expectations for the depth to the '410' in the cold Siberian shield. Chemical heterogeneity (i.e. spatial variation in Fe#) may further contribute to the seismic scattering, and will tend to disperse the metamorphic reactions spatially.

(2) The upper mantle at depths around the Transition Zone may be close to a pyrolitic composition with a content of about 60% olivine and 40% garnet and pyroxenes [4]. The pyroxenes will dissolve in the garnet phase to form the mineral majorite from depths of around 300 km, but primarily deeper than 350 km, such that complete conversion of the pyroxenes to garnet is achieved at a depth of ~460 km (Fig. 5D) [36]. The seismic velocity and density are higher in garnet than in pyroxenes, such that the metamorphic reaction causes marked positive velocity gradients in the depth interval from c. 300 to 460 km [4]. The seismic reflectivity from around the top of the Transition Zone is observed in approximately the same depth interval and it may be explained by local accumulations of high garnet concentration within the pyrolitic mantle rocks. The very few xenoliths reported from depths around the '410' show clear indication of the transformation of pyroxenes into majorite although, because of the sparse sampling at these extreme depths, no conclusions can be drawn regarding the scale lengths of the resulting inhomogeneity [34,37]. The transformation takes place mainly at depths below 400 km (i.e. the transformation curve is very steep above ~400 km depth). This indicates that this metamorphic reaction cannot be the sole reason for the seismic observations. However, the garnet transformation may explain much of the heterogeneity that is modelled inside the Transition Zone below the 410 discontinuity.

(3) The seismic observations show that the interval around the '410' is highly heterogeneous. Our modelling shows that scale lengths on the order of 20 by 5 km are consistent with the data. It may be unclear how the required heterogeneous mantle zone first came into existence. Subducted oceanic plates may create initial heterogeneity above the '410', in particular if they flatten in this depth interval. Recent tomographic models indicate

that subducting plates may pass through the Transition Zone to accumulate and equilibrate in the depth range of 600–1000 km [38]. However, the examples of slabs penetrating the Transition Zone are all from areas where relatively old oceanic plates are subducted. Young oceanic plates may equilibrate at a much shallower level. The phase transformation from α to β spinel at the top of the Transition Zone creates a density increase which may cause neutral buoyancy of some subducted plates at this depth level [39,40]. There is increasing evidence that the mantle is heterogeneous at various depth levels, which has been taken as evidence for equilibration of subducted slabs at most depth intervals in the mantle [5]. As such, the seismic heterogeneity that we observe may represent a depth level of a long-term accumulation of subducted oceanic lithosphere, which was young at the time of subduction and, therefore, equilibrated at the top of the Transition Zone. In any case, weak initial heterogeneity above the '410' from subducted plates may have initiated the metamorphic processes of pre-existing mantle minerals and, probably, also contributes to the observed seismic scattering.

The effect of water in the mantle rocks around the Transition Zone is to widen the depth range of the metamorphic changes, even for relatively small amounts of water [41]. This widening is gradual, and substantial fractions of the rocks are affected only close to the depth of the dry transformation. Less than 20% of the minerals are affected 17 km above the dry transition depth for an initial H_2O content of 1000 ppm in olivine [41]. Changes in frequency content of receiver functions from the Mediterranean area were recently interpreted in terms of metamorphic reactions caused by the presence of water around the '410' [42]. However, we observe a sharp onset of the seismic reflectivity from $\sim$80 km above the '410', which is contrary to the predicted gradual change in the metamorphic reactions caused by the presence of water. It is therefore unlikely that the presence of water is the main cause of the observed heterogeneity.

Analysis of multiply reflected seismic phases between the surface and the '410' for ScS phases has indicated the presence of a c. 80 km thick zone of low shear wave velocity above the mantle Transition Zone in eastern Siberia [26]. This has been explained in terms of silicate melts, which accumulate on top of the Transition Zone because of their high density. It is possible that this phenomenon contributes to the reflectivity, but it does not affect the depth of the phase transformation from olivine (α) to β spinel. The presence of the melts may enhance the heterogeneity of the zone, but it does not explain the observations of a sharp onset of the reflectivity.

5. Conclusion

The observed strong seismic reflectivity in all available record sections from Siberia and North America originates from a depth interval around the top of the mantle Transition Zone. It requires a heterogeneous mantle zone to scatter the incident seismic waves. The heterogeneous depth interval may be understood in terms of a widening of the α–β–γ phase transformation of the olivine part of the mantle rocks, caused by a higher iron content in this depth interval than hitherto estimated and observed in mantle xenoliths from shallower levels. The pyroxene to garnet (majorite) transformation probably contributes to the heterogeneity, in particular in the Transition Zone below the '410'. Both effects are supported by analysis of xenoliths from around the top of the Transition Zone. The presence of fluids or silicate melts may enhance the observed reflectivity but cannot explain all the observed phenomena. Heterogeneity from subducted oceanic slabs that equilibrated at the appropriate depth level may also contribute to the observed, strong seismic scattering.

Acknowledgements

This research was supported by the Carlsberg Foundation, the Danish Natural Science Research Council and the Polish State Committee of Scientific Research. The supercomputer facilities at the Danish Center for Scientific Computing (DCSC) were used for the finite-difference calculations.

J.O. Robertsson kindly provided the visco-elastic finite-difference codes. We are grateful to D.L. Anderson and two anonymous reviewers for instructive comments on an earlier version of the manuscript. *[SK]*

References

[1] R.D. v.d. Hilst, S. Widiyantoro, E.R. Engdahl, Evidence for deep mantle circulation from global tomography, Nature 386 (1997) 578–584.
[2] P.J. Tackley, Mantle convection and plate tectonics: Toward an integrated physical and chemical theory, Science 288 (2000) 2002–2007.
[3] D.L. Anderson, Top-down tectonics?, Science 293 (2002) 2016–2018.
[4] A.E. Ringwood, Phase transformations and their bearing on the constitution and dynamics of the mantle, Geochim. Cosmochim. Acta 55 (1991) 2083–2110.
[5] G.R. Helffrich, B.J. Woods, The Earth's mantle, Nature 412 (2001) 501–507.
[6] D.L. Anderson, J.D. Bass, Transition region of the Earth's upper mantle, Nature 320 (1986) 321–328.
[7] D.L. Anderson, Theory of the Earth, Blackwell Scientific, Boston, MA, 1989, 366 pp.
[8] A.F. Birch, Elasticity and constitution of the earth's interior, J. Geophys. Res. 57 (1952) 227–286.
[9] D.L. Anderson, Phase changes in the upper mantle, Science 157 (1967) 1165–1173.
[10] T. Katsura, E. Ito, The system Mg_2SiO_4-Fe_2SiO_4 at high pressures and temperatures; precise determination of stabilities of olivine, modified spinel, and spinel, J. Geophys. Res. B Solid Earth Planets 94 (1989) 15,663–15,670.
[11] M. Akaogi, E. Ito, A. Navrotsky, Olivine-modified spinel-spinel transitions in the system Mg_2SiO_4-Fe_2SiO_4; calorimetric measurements, thermochemical calculation, and geophysical application, J. Geophys. Res. B Solid Earth Planets 94 (1989) 15,671–15,685.
[12] H.M. Benz, J.E. Vidale, Sharpness of upper-mantle discontinuities determined from high-frequency reflections, Nature 365 (1993) 147–150.
[13] F. Neele, Sharp 400-km discontinuity from short-period P reflections, Geophys. Res. Lett. 23 (1996) 419–422.
[14] C.R. Bina, B.J. Wood, Olivine-spinel transitions; experimental and thermodynamic constraints and implications for the nature of the 400-km seismic discontinuity, J. Geophys. Res. B Solid Earth Planets 92 (1987) 4853–4866.
[15] G.R. Helffrich, B.J. Wood, 410 km discontinuity sharpness and the form of the olivine alpha-beta phase diagram; resolution of apparent seismic contradictions, Geophys. J. Int. 126 (1996) F7–F12.
[16] G. Bock, J. Gossler, W. Hanka, R. Kind, G. Kosarev, N. Petersen, K. Stammler, L. Vinnik, On the seismic discontinuities in the upper mantle, in: S. Franck, J. Ahrens Thomas (Eds.), Structure, Composition and Evolution of the Earth's Interior, Phys. Earth Planet. Inter. 92 (1995) 39–43.
[17] K. Stammler, R. Kind, G.L. Kosarev, A. Plesinger, J. Horalek, L. Qiyuan, L.P. Vinnik, Broadband observations of PS conversions from the upper mantle in Eurasia, Geophys. J. Int. 105 (1991) 801–804.
[18] M.C. Walck, The P-wave upper mantle structure beneath an active spreading centre: the Gulf of California, Geophys. J. R. Astron. Soc. 76 (1984) 697–723.
[19] J.E. Vidale, X.Y. Ding, S.P. Grand, The 410-km-depth discontinuity; a sharpness estimate from near-critical reflections, Geophys. Res. Lett. 22 (1995) 2557–2560.
[20] H. Thybo, E. Perchuc, N.I. Pavlenkova, Two reflectors in the 400 km depth range revealed from peaceful nuclear explosion seismic sections, in: K. Fuchs (Ed.), Upper Mantle Heterogeneities from Active and Passive Seismology, NATO Science Series. Partnership Sub-series 1, Disarmament Technologies 17, Kluwer Academic, Dordrecht, 1997, pp. 97–103.
[21] W.D. Mooney, T.M. Brocher, Coincident seismic reflection/refraction studies of the continental lithosphere; a global review, Rev. Geophys. 25 (1987) 723–742.
[22] D.D. Sultanov, J.R. Murphy, K.D. Rubinstein, A seismic source summary for Soviet peaceful nuclear explosions, Bull. Seismol. Soc. Am. 89 (1999) 640–647.
[23] B.T. Lewis, R.P. Meyer, A seismic investigation of the upper mantle to the west of Lake Superior, Bull. Seismol. Soc. Am. 58 (1968) 565–596.
[24] T. Melbourne, D. Helmberger, Fine structure of the 410-km discontinuity, J. Geophys. Res. 103 (1998) 10,091–10,102.
[25] E. Perchuc, H. Thybo, Variation in depth to the 410 km discontinuity in North America from El Paso earthquakes. EOS, Trans Am. Geophys. Union Fall Meet. (2001).
[26] J. Revenaugh, S.A. Sipkin, Seismic evidence for silicate melt atop the 410-km mantle discontinuity, Nature 369 (1994) 474–476.
[27] J.O. Robertsson, J.O. Blanch, W.W. Symes, Viscoelastic finite-difference modeling, Geophysics 59 (1994) 1444–1456.
[28] L. Nielsen, H. Thybo, A.V. Egorkin, Implications of seismic scattering below the 8° discontinuity along PNE seismic profile Kraton, Tectonophysics 358 (2002) 135–150.
[29] L. Nielsen, H. Thybo, L. Solodilov, Seismic tomographic inversion of Russian PNE data along profile Kraton, Geophys. Res. Lett. 26 (1999) 3413–3416.
[30] B.L.N. Kennett, E.R. Engdahl, Traveltimes for global earthquake location and phase identification, Geophys. J. Int. 105 (1991) 429–465.
[31] K. Holliger, A.R. Levander, A stochastic view of lower crustal fabric based on evidence from the Ivrea Zone, Geophys. Res. Lett. 19 (1992) 1153–1156.
[32] H. Bijwaard, W. Spakman, E.R. Engdahl, Closing the gap between regional and global travel time tomography, J. Geophys. Res. B Solid Earth Planets 103 (1998) 30,055–30,078.

[33] D.V. Helmberger, G.R. Engen, Upper mantle shear structure, J. Geophys. Res. 79 (1974) 4017–4028.
[34] V. Sautter, S.E. Haggerty, S. Field, Ultradeep (>300 kilometers) ultramafic xenoliths; petrological evidence from the transition zone, Science 252 (1991) 827–830.
[35] C.B. Agee, Phase transformations and seismic structure in the upper mantle and transition zone, in: J. Hemley Russell (Ed.), Ultrahigh-pressure Mineralogy; Physics and Chemistry of the Earth's Deep Interior, Rev. Mineral. 37 (1998) 165–203.
[36] T. Irifune, An experimental investigation of the pyroxene-garnet transformation in a pyrolite composition and its bearing on the constitution of the mantle, Phys. Earth Planet. Inter. 45 (1987) 324–336.
[37] K.D. Collerson, S. Hapugoda, B.S. Kamber, Q. Williams, Rocks from the mantle transition zone majoite-bearing xenoliths from Malaita, Southwest Pacific, Science 288 (2000) 1215–1223.
[38] Y.etal. Fukao, Stagnant slabs in the upper and lower mantle transition region, Rev. Geophys. 39 (2001) 291–323.
[39] L. Wen, D.L. Anderson, Th fate of slabs inferred from seismic tomgraphy and 130 Mill. years of subduction, Earth Planet. Sci. Lett. 133 (1995) 185–187.
[40] S. van der Lee, G. Nolet, Seismic image of the subducted trailing fragments of the Farallon Plate, Nature 386 (1997) 266–269.
[41] B.J. Wood, The effect of H_2O on the 410-kilometer seismic discontinuity, Science 268 (1995) 74–76.
[42] M. van der Meijde, F. Marone, D. Giardini, S. van der Lee, Seismic evidence for water deep in Earth's upper mantle, Science 300 (2003) 1556–1558.